Synthetic Metals 197 (2014) 188–193

Contents lists available at ScienceDirect

Synthetic Metals

journal homepage: www.elsevier.com/locate/synmet

Di-*n*-alkylphosphinic acids as coadsorbents for metal-free organic dye-sensitized solar cells

Jingzhe Li[a], Fantai Kong[a,*], Guohua Wu[a], Wangchao Chen[a], Fuling Guo[a], Bing Zhang[b], Jianxi Yao[b], Shangfeng Yang[c], Songyuan Dai[b,a,*], Xu Pan[a]

[a] Key Laboratory of Novel Thin Film Solar Cells, Institute of Plasma Physics, Chinese Academy of Sciences, Hefei 230031, PR China
[b] School of Renewable Energy, North China Electric Power University, Beijing 102206, PR China
[c] Hefei National Laboratory for Physical Sciences at Microscale, Department of Materials Science and Engineering, University of Science and Technology of China (USTC), Hefei 230026, PR China

ARTICLE INFO

Article history:
Received 11 May 2014
Received in revised form 21 August 2014
Accepted 16 September 2014

Keywords:
Dye-sensitized solar cells
TiO_2/dye/electrolyte interface
Coadsorbent
Di-*n*-alkylphosphinic acid
Charge recombination

ABSTRACT

Three di-*n*-alkylphosphinic acids (DPAs) with different chain lengths (1, 8, 16) were adopted as coadsorbents in dye-sensitized solar cells (DSCs) with organic sensitizer D149. The adsorption behavior of these coadsorbents on nanoporous TiO_2 surface through P—O—Ti bond was confirmed by FT-IR spectra. And the performance of all devices was detected on the basis of photocurrent–voltage (*J*–*V*) characteristics and electrochemical impedance spectroscopy (EIS). It was found that the amount of dye adsorption gradually decreased with increasing alkyl chain length of DPAs, which was contributed to the competitive adsorption between dye D149 and coadsorbents. In spite of this, di-*n*-hexadecylphosphinic acid (DHdPA) performed best both in the improvement of short-circuit current density (J_{sc}) and open-circuit voltage (V_{oc}). The increase of open-circuit photovoltage was ascribed to the negative movement of the conduction band edge and the retardation of electron recombination. Although the dye adsorption amount reduced to a great degree, the break up of dye aggregation mainly contribute to the enhancement of short-circuit current density. The overall conversion efficiency was further improved from 5.53% to 6.09% with DHdPA as the coadsorbent for D149 based device.

1. Introduction

Dye-sensitized solar cells (DSCs) have been intensively studied and developed in the past decades due to the potential of low-cost production, high efficiency and simple fabrication process [1,2]. In recent years, great progress has been made on DSCs for further improving the power conversion efficiency [3]. However, there is still a large gap between the achieved efficiency and the theoretical value [3–5], especially the energy loss in TiO_2/dye/electrolyte interface caused by the charge recombination between electrons in the conduction band of TiO_2 and acceptors in the electrolyte [6,7]. Thus, great efforts have been made to perfect this interface through various methods [8–14], such as TiO_2 surface modification with $TiCl_4$ solution [9], acid treatment [10] and metal oxide blocking layers [11], additives in electrolyte [12,13], and the incorporation of coadsorbent in dye bath [14]. Among them, coadsorbent mixed with dye during the sensitization step is considered to be a simple and effective method [15]. Various coadsorbents, such as cholic acid derivatives [16,17], decylphosphonic acid [18], bis(3,3-dimethylbutyl)phosphinic acid (DINHOP) [19], have been widely used in co-adsorption with sensitizer onto the TiO_2 surface. Generally, ruthenium-dye based DSCs are co-adsorbed with carboxylic acid or phosphonic acid [19–23]. While for most organic dyes, cholic acid (CA) derivatives are often chosen as coadsorbents to break up the dye aggregation, thereby significantly improve V_{oc} and J_{sc} [24,25].

As reported, there is a positive influence of phosphinic acids on the performance of ruthenium-dye based DSCs [19,26]. However, the effect of alkyl chain length of DPAs on the device performance has not been clearly addressed; moreover the combination of phosphinic acids with organic-dye based devices has not been reported in the literature. Metal-free indoline organic dyes (such as D149) have proved to be highly efficient in DSCs, whereas

* Corresponding authors at: Key Laboratory of Novel Thin Film Solar Cells, Institute of Plasma Physics, Chinese Academy of Sciences, 350 Shushanhu Road, P.O. Box 1126, Hefei 230031, Anhui, PR China. Tel.: +86 551 65593222; fax: +86 551 65591377.
E-mail addresses: ljz132006@163.com (J. Li), kongfantai@163.com (F. Kong), wgh1988@yeah.net (G. Wu), chenwc0922@yeah.net (W. Chen), guofuling198702@163.com (F. Guo), mpezb310@gmail.com (B. Zhang), jianxiyao@ncepu.edu.cn (J. Yao), sfyang@ustc.edu.cn (S. Yang), sydai@ipp.ac.cn (S. Dai), mars_dark@hotmail.com (X. Pan).

http://dx.doi.org/10.1016/j.synthmet.2014.09.023
0379-6779/

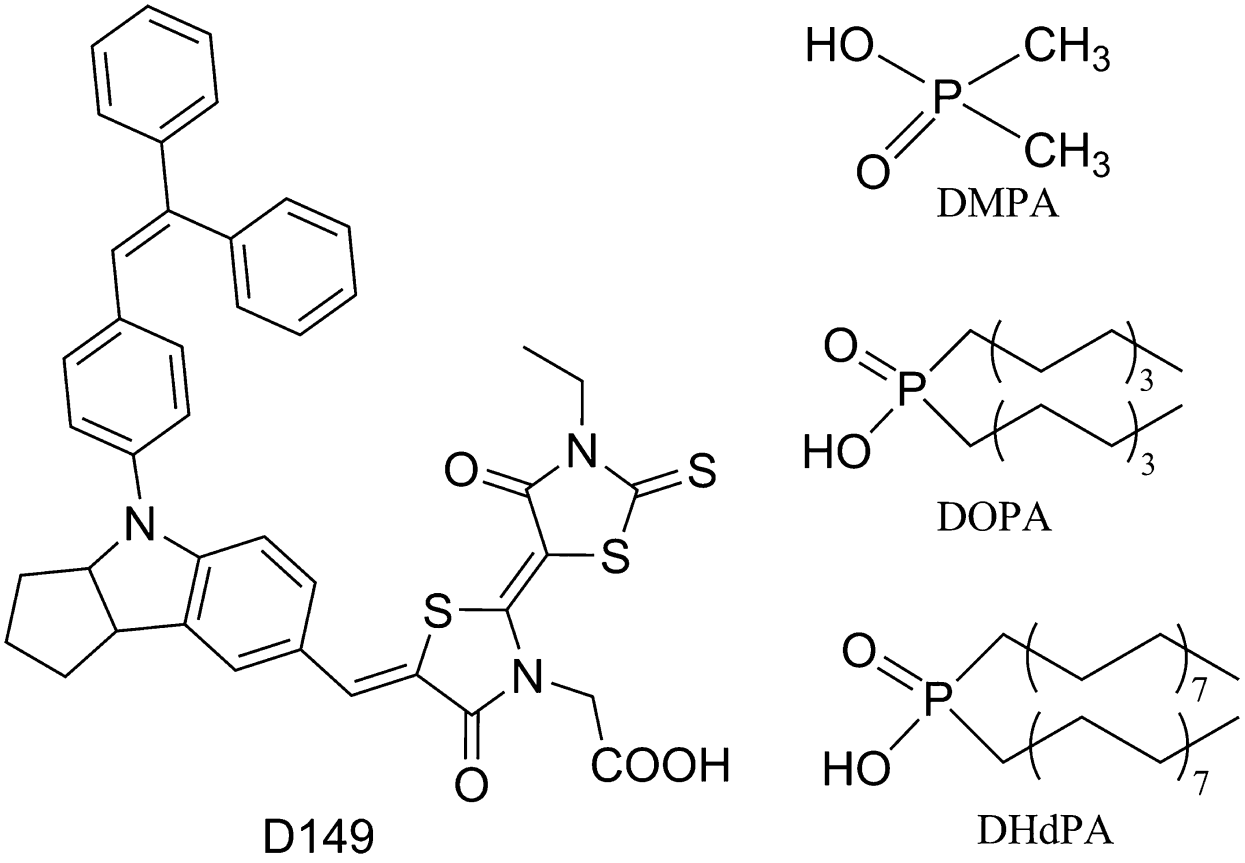

Fig. 1. Molecular structures of D149 dye, DMPA, DOPA and DHdPA.

aggregation of this kind of dye molecules usually occurs along with the strong intermolecular interaction. The choice of coadsorbents in indoline-dye based DSCs in many works is a typical way to dissociate dye aggregation and thus to improve device efficiency [24]. In the present work, three di-*n*-alkylphosphinic acids with different alkyl chains (1, 8, 16, the molecular structures are displayed in Fig. 1) were used as coadsorbents with metal-free indoline sensitizer D149. The performance of DSCs by DPAs with different alkyl chains was examined and investigated in detail.

2. Experiment

2.1. Reagents and synthesis

D149 dye, dimethylphosphinic acid (DMPA), anhydrous lithium iodide and iodine (I_2) were purchased from Aldrich. Di-*n*-octylphosphinic acid (DOPA) and di-*n*-hexadecylphosphinic acid (DHdPA) were synthesized by a literature method [27]. In a 50 ml three-necked round-bottom flask, a mixture of 1-octene (3.36 g, 30 mmol), hypophosphorous acid (50 w/w%, 1.06 g, 10 mmol H_3PO_2), benzoyl peroxide (0.07 g, 0.3 mmol) and 1, 4-dioxane (20 ml) was refluxed for 22 h. After cooling to room temperature, a white solid crude product was obtained by extraction and acidification of the organic layer. The crude product was recrystallized from *n*-heptane to yield white powders (0.27 g, 9.4%). mp: 84.8 °C; ^{1}H NMR (500 MHz, $CDCl_3$): δ/ppm = 1.65 (m, 4H, $2CH_2$-P), 1.59 (m, 4H, $2CH_2$), 1.24–1.4 (m, 20H, $10CH_2$), 0.88 (t, 6H, $2CH_3$, J = 7 Hz); FT-IR (KBr): ν 969, 1152, 1470, 2919 cm^{-1}; FTMS-ESI (m/z): calcd for $[M-H]^-$: 289.2296, found: 289.2313. The synthesis and post-treatment procedure of DHdPA was identical to that of DOPA. As confirmed by ^{1}H NMR, FT-IR and FTMS-ESI. Analysis: mp: 101.76 °C; ^{1}H NMR (500 MHz, $CDCl_3$): δ/ppm = 1.65 (m, 4H, $2CH_2$-P), 1.59 (m, 4H, $2CH_2$), 1.24–1.38 (m, 52H, $26CH_2$), 0.88 (t, 6H, $2CH_3$, J = 7 Hz); FT-IR (KBr): ν 968, 1145, 1470, 2919 cm^{-1}; FTMS-ESI (m/z): calcd for $[M-H]^-$: 513.4800, found: 513.4793.

2.2. Fabrication of DSCs

The colloidal TiO_2 nanoparticles were synthesized by hydrolysis of titanium (IV) isopropoxide as described elsewhere [28]. Then the colloidal TiO_2 paste was coated on FTO conductive glass substrate (TEC-15, LOF) by screen printing. The films were dried at room temperature for 5 min and then sintering at 450 °C under air for 30 min. A transparent TiO_2 thin-film electrode was obtained and the thickness of the TiO_2 films was about 12 μm and the active area was 0.5 cm × 0.5 cm = 0.25 cm^2. The thickness of film was measured by surface profilometer (XP-2, AMBIOS Technology Inc., USA). Then the TiO_2 films were immersed in a sensitizing solution at room temperature for 12 h. The optimized solutions contained 0.5 mM D149 dye and coadsorbent DMPA, DOPA, DHdPA (molar ratio as 8:1) in the chloroform. The platinized counter electrodes were prepared by spraying H_2PtCl_6 solution on FTO, followed by heating at 410 °C for 20 min. The two electrodes were sealed with a 45 μm thermal adhesive film (Surlyn, DuPont) and the internal space between the two was filled with the electrolyte through a hole drilled in the counter electrode which was subsequently sealed by surlyn adhesive film and a cover glass. The organic electrolyte was made up of 0.1 M I_2, 0.1 M lithium iodide and 0.5 M 1,2-dimethyl-3-propylimidazolium iodide (DMPII) in acetonitrile (ACN).

2.3. Analytical measurements

The photocurrent–voltage (J–V) characteristics of the DSC were achieved by a 3A grade solar simulator (Newport, USA, 94043A,

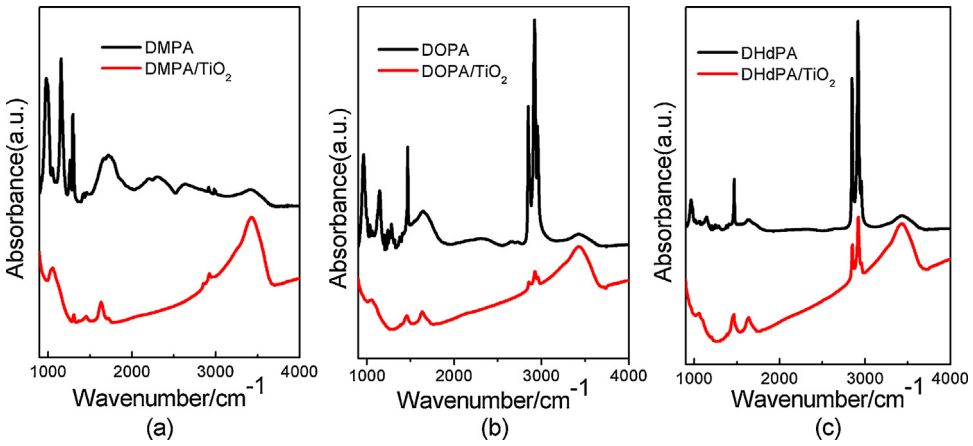

Fig. 2. FT-IR spectra of DMPA, DOPA, and DHdPA using solid samples and on mesoporous TiO_2 films.

calibrated with a standard crystalline silicon solar) under AM 1.5 (100 mW cm^{-2}) illumination. Monochromatic incident photon to current conversion efficiency (IPCE) was recorded using a computerized setup consisting of a 2931-C dual channel power meter and a 300 W xenon lamp, followed by a 1/4 m monochromator as a light source. IM6eX Electrochemical Workstation (Germany, Zahner Company) was employed to carry out the electrochemical impedance spectroscopy (EIS) measurements at reverse biases in dark. The amplitude of the alternative signal was 5 mV, with the frequency range from 1 MHz to 5 mHz. The FT-IR spectra for all the samples were measured by using a NICOLET8700 FT-IR spectrometer (USA, Thermo Fisher Scientific) using KBr pellets. The estimation of dye loading amount was taken on a UV–vis spectrophotometer (U-3900H, Hitachi, Japan.). ^{1}H NMR spectra were measured by a Bruker Avance 500 spectrometer with the chemical shifts against tetramethylsilane (TMS). Electrospray ionization mass spectrometry (ESI-MS) spectra were obtained from a LTQ Orbitrap XL Mass Spectrometer.

3. Results and discussion

Fig. 2 shows the FT-IR spectra of three coadsorbents and the mesoporous TiO_2 stained with DMPA, DOPA, DHdPA. According to the spectra of coadsorbents, DMPA presents the characteristic absorption bands at 979 cm^{-1} and 1171 cm^{-1} which are attributed to ν(P—O) and ν(P═O). Similarly, ν(P—O) and ν(P═O) loading at the peak of 969 cm^{-1} and 1152 cm^{-1} for DOPA, and loading at the peak of 968 cm^{-1} and 1145 cm^{-1} for DHdPA, respectively. When DMPA was adsorbed onto the TiO_2 films, a new peak appeared at 1060 cm^{-1} related to the stretching vibration of P—O—Ti of DMPA/TiO_2 in the FT-IR spectra [29]. Similar to DMPA/TiO_2, the new peak at 1056 cm^{-1} related to P—O—Ti bond of DOPA/TiO_2 and DHdPA/TiO_2. These results demonstrate that the three coadsorbents are successfully bound to the surface of TiO_2 electrodes *via* the phosphinate group.

Fig. 3 shows the absorption spectra of the D149 dye and the D149 dye with coadsorbents adsorbed onto a 3 μm TiO_2 film. The UV–vis spectrum for the TiO_2 film absorbed with dye only shows the absorbance peak at about 530 nm (λ_{max}) which exhibits a larger absorption than the TiO_2 films absorbed with dye and DPAs. When the dye with DPAs was adsorbed onto the TiO_2 films, the amount of dye adsorption was gradually decreased with the two alkyl chain length increasing. This is attributed to the competition of the DPAs with dye D149 for the limited adsorption sites on TiO_2 surface during the sensitization process. We also measured the amount of dye adsorption by desorbing dye in DMF solution followed by spectroscopic analysis (Table 1). After measuring the desorbed dye solution

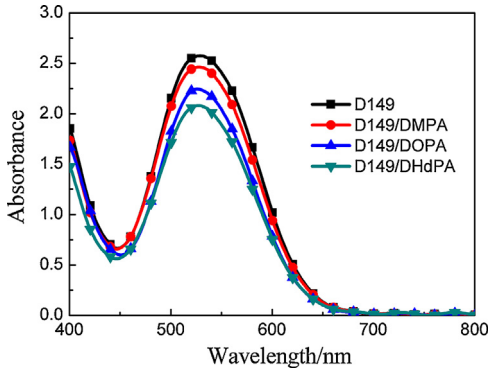

Fig. 3. UV–vis spectra of 3 μm TiO_2 films sensitized by D149 with different coadsorbents.

from the 12 μm TiO_2 films (same thickness with the electrode), we found that the amount of dye on the TiO_2 films was decreased compared with D149/TiO_2, which leading to a 5%, 14%, and 20% drop in D149/DMPA/TiO_2, D149/DMPA/TiO_2, D149/DHdPA/TiO_2, respectively. The results indicate that all coadsorbents used in this study decrease the amount of dye loaded, which have a great relationship with the alkyl chain length of DPAs.

Fig. 4 shows the IPCE spectra as a function of the light wavelength. The corresponding photocurrent density-voltage (*J–V*) curves for the DSCs using DPAs under one sun illumination (AM 1.5) are shown in Fig. 5 and the photovoltaic performance is displayed in Table 1. Specifically, DMPA demonstrated the lowest IPCE value corresponding to the poorest conversion efficiency among

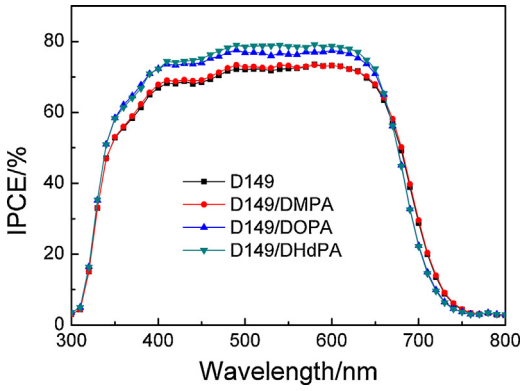

Fig. 4. IPCE spectra for devices sensitized by D149 with different coadsorbents.

Table 1
Photovoltaic performance of devices sensitized by D149 with different coadsorbents.

Devices	V_{oc} (V)	J_{sc} (mA cm^{-2})	FF	Efficiency (%)	Adsorption[a] (10^{-7} mol cm^{-2})
D149	0.591	14.23	0.65	5.53	2.07
D149/DMPA	0.593	14.24	0.66	5.60	1.95
D149/DOPA	0.618	14.80	0.64	5.81	1.79
D149/DHdPA	0.625	15.14	0.64	6.09	1.65

[a] Adsorption amount per unit area of TiO_2 film.

the three treated devices. But with the alkyl chain length increasing, the devices performance treated by DOPA and DHdPA were significantly improved. The device without coadsorbent only exhibited a J_{sc} of 14.23 mA cm^{-2}, V_{oc} of 589 mV, and conversion efficiency of 5.53%. Except DMPA, co-grafting with DOPA or DHdPA, both the J_{sc} and V_{oc} were increased, and the overall conversion efficiency was calculated to be improved by 5.06% and 10.12% as compared with device without coadsorbent, respectively. The *J–V* curves of the devices under dark conditions (Fig. 5) suggested that DHdPA as coadsorbent suppressed the dark current more effectively than DMPA and DOPA.

IPCE spectra show the same tendency as observed in *J–V* curves. IPCE is governed by light-harvesting efficiency (LHE), charge injection efficiency (φ_{inj}) and charge collection efficiency (η_c) as the following Eq. (1) [30]:

$$\mathrm{IPCE}(\lambda) = \mathrm{LHE}(\lambda)\varphi_{inj}\eta_c \quad (1)$$

LHE is determined by the extinction coefficient and the density adsorption of the sensitizer. From the UV–vis absorption analysis, even though the amount of dye loaded on TiO_2 films decreased largely with DHdPA, the IPCE was higher than devices with other two coadsorbents. This result indicates that the light harvesting by the sensitizer may not be the limiting factor in device performance. In terms of electron injection, coadsorbent of organic molecules could break up dye aggregation and increase electron injection, resulting in an enhanced photocurrent which has been reported in the literature [25]. Therefore, in this study phosphinic acid with long alkyl chains may efficiently reduce the D149 dye aggregation, and the effect may not appeared by DMPA with only one methyl. Retardation of charge recombination has been proved to enhance the charge collection efficiency [30] which was investigated in detail later using EIS. In summary, the superior photocurrent of the device treated by DHdPA may due to the improvements both of φ_{inj} and η_c, despite lowest dye loading.

In order to analysis whether the first dye coating is necessary, the complementary experiment was carried on. The TiO_2 electrodes were firstly immersed into D149 dye (0.5 mmol/L) solution for 12 h, after that washed with chloroform, and then transferred to different

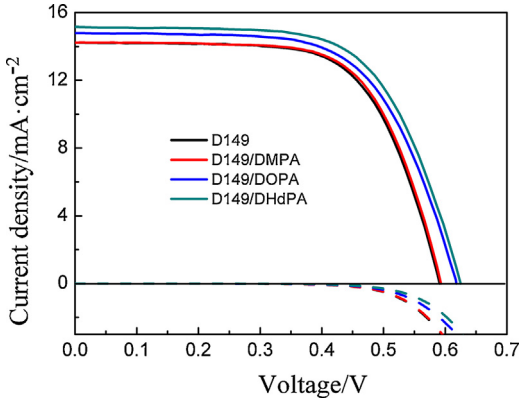

Fig. 5. *J–V* characteristics for devices sensitized by D149 with different coadsorbents under AM1.5 simulated illumination (solid line) and in the dark (dashed line).

DPAs solution for 12 h (0.0625 mmol/L), respectively. After sensitization process, the photoanode electrodes were assembled into devices as described in the manuscript. The photovoltaic performance is displayed in Table 2. As showed in Table 2, the devices treated by DPAs after the sensitization step are performed poorer and the amount of dye adsorption was decreased greatly compared with D149 dye only. During the process treated by DPAs, the dye desorbed obviously which is contributed to the coadsorbents' P—O—Ti bond strongly bind with TiO_2. DMPA with smallest molecular structure can easily penetrate through dyes than the other two coadsorbents, therefore device **B** demonstrated the lowest conversion efficiency and dye adsorption. In summary, our investigation of DPAs which are applied after dye adsorption is unnecessary.

Fig. 6(a) shows the Nyquist plot of EIS obtained in the dark under a bias voltage of −0.60 V. Two semi-circles are observed with gradually increasing frequency, the first semicircle at high-frequency is related to the charge transfer at the platinum counter electrode/electrolyte interface, and the low-frequency semicircle corresponds to the electron recombination at the TiO_2/electrolyte interface [22]. To further investigate the effect of coadsorbents on V_{oc}, EIS was performed under dark conditions at different bias voltages between −0.50 V and −0.60 V. The chemical capacitance (C_μ) and interfacial charge transfer resistance (R_{CT}) were obtained by fitting the experimental data of all devices with an equivalent circuit presented in Fig. 6(a), where R_s was the system resistance, R_{PT} was charge-transfer processes occurring at the Pt/electrolyte interface and R_{CT} is charge transfer resistance occurring at TiO_2/electrolyte interface.

Generally, the value of V_{oc} is theoretically determined by the difference between the Fermi level of TiO_2 ($E_{F,n}$) and the redox potential of the redox couple I_3^-/I^- (E_{redox}). On the other hand, the $E_{F,n}$ of TiO_2 can be described as Eq. (2) [31]:

$$E_{F,\mathrm{n}} = E_{CB} + k_B T \ln\left(\frac{n_c}{N_c}\right) \quad (2)$$

where k_B is the Boltzmann constant, T is the experimental temperature (293 K in this work), n_c is the free electron density in TiO_2, and N_c is the total number of accessible states in the semiconductor. E_{CB} is the conduction band edge of TiO_2. Supposing E_{redox} to be constant, V_{oc} will be determined by the position of the conduction band edge and the electrons concentration of TiO_2. C_μ is a significant parameter to evaluate the influence of coadsorbent on E_{CB}, which can be expressed as follows by Eq. (3) [32]:

$$C_\mu = \frac{e^2}{k_B T}\exp\left[\frac{\alpha}{k_B T}(E_{redox} + eV - E_{CB})\right] \quad (3)$$

where e is elementary charge, α is a constant related to the distribution of electronic states below the conduction band and V is the bias voltage in the measurement. So the position of the E_{CB} can be estimated by analyzing the value of C_μ at a certain bias voltage. Fig. 6(b) shows the C_μ value of different devices under different bias. The values are in the order of D149 > D149/DMPA > D149/DOPA ≈ D149/DHdPA, indicating that the conduction band of the TiO_2 negatively shifts and increase the V_{oc} of the device when treating with DPAs. The movement E_{CB} for the above devices is partially responsible for the variation of V_{oc}.

Table 2
Photovoltaic performance of devices sensitized by D149 with different coadsorbents.

Devices	TiO_2 electrodes treatment	V_{oc} (V)	J_{sc} (mA cm^{-2})	FF	Efficiency (%)	Adsorption[a] (10^{-7} mol cm^{-2})
A	Dye only 12 h	0.591	14.23	0.65	5.53	2.07
B	Dye 12 h, then DMPA 12 h	0.441	3.533	0.65	1.01	0.07
C	Dye 12 h, then DOPA 12 h	0.584	10.31	0.66	3.97	0.74
D	Dye 12 h, then DHdPA 12 h	0.590	11.17	0.65	4.28	1.11

[a] Adsorption amount per unit area of TiO_2 film.

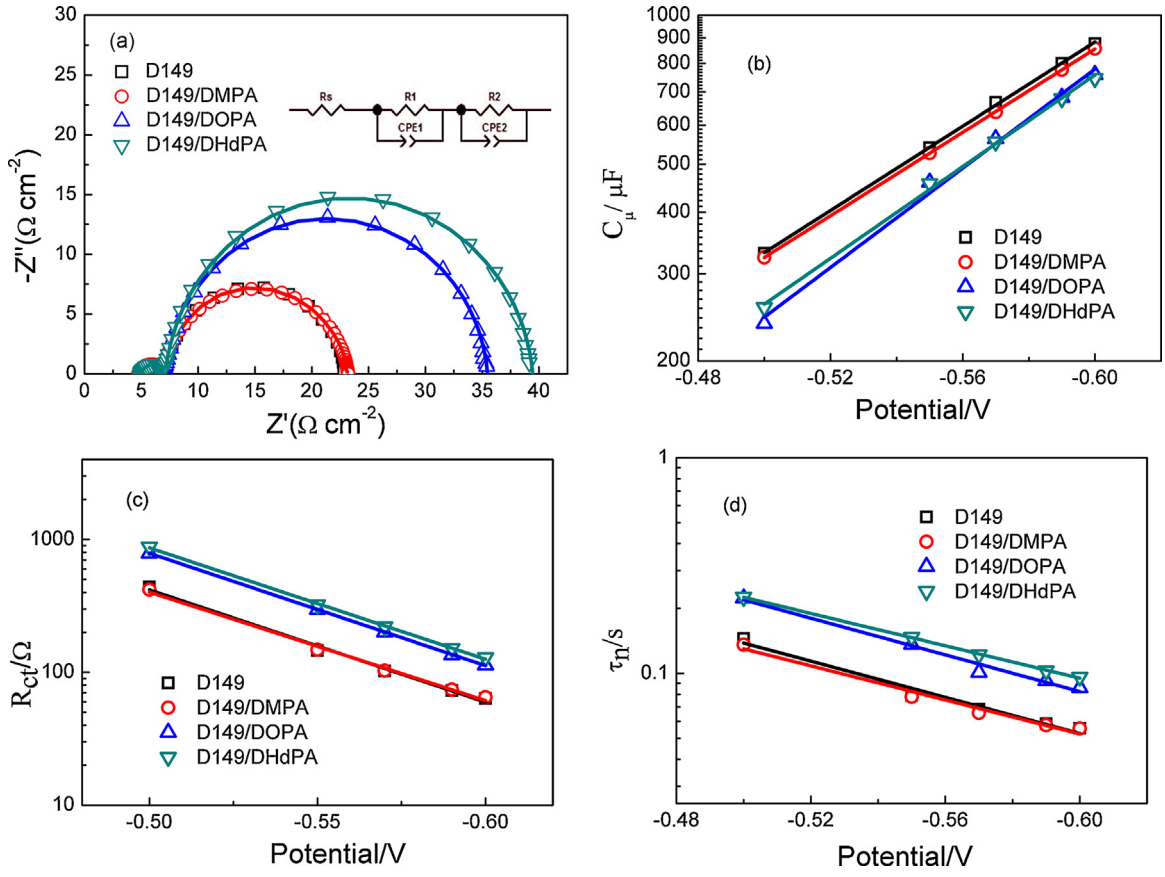

Fig. 6. Electrochemical impedance spectroscopy of devices with different coadsorbents (a) Nyquist plots; (b) C_μ; (c) R_{CT} and (d) τ_n versus bias voltages of DSCs.

The charge recombination resistance R_{CT} at the interface between TiO_2 and electrolyte redox species was further investigated from impedance spectra which was expressed by Eq. (4) [33]:

$$R_{CT} = R_0 \exp\left(-e\frac{\beta V}{k_B T}\right) \quad (4)$$

where β is the transfer coefficient which corresponds to the reciprocal value of diode quality factor, R_0 is constant. The R_{CT} is related to the charger recombination rate, which means that larger R_{CT} leads to smaller charge recombination rate. Compared to the other devices, DHdPA shows the largest value at any given bias voltage as presented in Fig. 6(c). The phosphinic acid with long alkyl chains acted as an efficient passivating layer for the retarding charge recombination between the electrons in TiO_2 surface and I_3^-, thus could enlarging the η_c values discussed before. Electron lifetime (τ_n) plotted in Fig. 6(d) which could be calculated from the C_μ and R_{CT} using the equation $\tau_n = C_\mu R_{CT}$ in fitting the EIS curves. DHdPA exhibits evidently enhanced electron lifetime in the four D149 based DSC devices. This order is consistent with the result obtained from charge transfer resistance Above all, the observations suggest that DHdPA as coadsorbent grafted with D149 dye is more effective than DOPA and DMPA in suppressing the recombination of electrons, which results in the simultaneous improvement in J_{sc} and V_{oc}.

4. Conclusion

In summary, the investigation of coadsorbents in metal-free organic dye DSCs is developed in this work by altering alkyl chain length of DPAs. Three coadsorbents (DMPA, DOPA, DHdPA) can successfully adsorb onto the TiO_2 surface via the phosphinate group as confirmed by FT-IR spectra. With the alkyl chain length increasing, the coverage of dye D149 on TiO_2 electrode gradually decreased which was attributed to the competition of DPAs with dye molecules under the optimized conditions. Di-*n*-hexadecylphosphinic acid (DHdPA) performed best both in the improvement of short-circuit current density and open-circuit voltage due to its more obvious steric hindrance effects. The bulky structure with two long hydrophobic alkyl chains effectively reduced the electron recombination which was also beneficial to diminish the dye aggregation. In contrast, dimethylphosphinic acid (DMPA) showed no positive effect on the performance of DSCs. Furthermore, DHdPA also caused the negative shift of the conduction

band edge of the TiO_2 film. As a result, the overall conversion efficiency was further improved by almost 10% compared with the device sensitized with D149 only.

Acknowledgements

This work was financially supported by the National Basic Research Program of China under grant no. 2011CBA00700, the National Natural Science Foundation of China under grant no. 21003130, the National High Technology Research and Development Program of China under grant nos. (2011AA050510, 2011AA050527), and the Program of Hefei Center for Physical Science and Technology no. 2012FXZY006.

References

[1] O'Regan, M. Grätzel, Nature 353 (1991) 737–740.
[2] M.K. Nazeeruddin, A. Kay, I. Rodicio, R. Humphrybaker, E. Muller, P. Liska, N. Vlachopoulos, M. Grätzel, J. Am. Chem. Soc. 115 (1993) 6382–6390.
[3] A. Yella, H.-W. Lee, H.N. Tsao, C. Yi, A.K. Chandiran, M.K. Nazeeruddin, E.W.-G. Diau, C.-Y. Yeh, S.M. Zakeeruddin, M. Grätzel, Science 334 (2011) 629–634.
[4] H.J. Snaith, Adv. Funct. Mater. 20 (2010) 13–19.
[5] B.J. Song, H.M. Song, I.T. Choi, S.K. Kim, K.D. Seo, M.S. Kang, M.J. Lee, D.W. Cho, M.J. Ju, H.K. Kim, Chem. Eur. J. 17 (2011) 11115–11121.
[6] S.Y. Huang, G. Schlichthorl, A.J. Nozik, M. Grätzel, A.J. Frank, J. Phys. Chem. B 101 (1997) 2576–2582.
[7] M. Duerr, A. Yasuda, G. Nelles, Appl. Phys. Lett. 89 (2006) 061110.
[8] S.E. Koops, B.C. O'Regan, P.R.F. Barnes, J. Am. Chem. Soc. 131 (2009) 4808–4818.
[9] M.Y. Song, D.K. Kim, S.M. Jo, D.Y. Kim, Synth. Met. 155 (2005) 635–638.
[10] Z.S. Wang, T. Yamaguchi, H. Sugihara, H. Arakawa, Langmuir 21 (2005) 4272–4276.
[11] E. Palomares, J.N. Clifford, S.A. Haque, T. Lutz, J.R. Durrant, J. Am. Chem. Soc. 125 (2003) 475–482.
[12] J. Zhao, F. Yan, L. Qiu, Y. Zhang, X. Chen, B. Sun, Chem. Commun. 47 (2011) 11516–11518.
[13] K. Mi-Jeong, P. Nam-Gyu, Appl. Surf. Sci. 258 (2012) 8915–8918.
[14] N. Kopidakis, N.R. Neale, A.J. Frank, J. Phys. Chem. B 110 (2006) 12485–12489.
[15] A. Kay, M. Grätzel, J. Phys. Chem. 97 (1993) 6272–6277.
[16] X. Ren, Q. Feng, G. Zhou, C.-H. Huang, Z.-S. Wang, J. Phys. Chem. C 114 (2010) 7190–7195.
[17] H. Chen, H. Huang, X. Huang, J.N. Clifford, A. Forneli, E. Palomares, X. Zheng, L. Zheng, X. Wang, P. Shen, B. Zhao, S. Tan, J. Phys. Chem. C 114 (2010) 3280–3286.
[18] P. Wang, S.M. Zakeeruddin, R. Humphry-Baker, J.E. Moser, M. Grätzel, Adv. Mater. 15 (2003) 2101–2104.
[19] M. Wang, X. Li, H. Lin, P. Pechy, S.M. Zakeeruddin, M. Grätzel, Dalton Trans. 45 (2009) 10015–10020.
[20] P. Wang, S.M. Zakeeruddin, R. Humphry-Baker, M. Gratzel, Chem. Mater. 16 (2004) 2694–2696.
[21] J. Lim, Y.S. Kwon, T. Park, Chem. Commun. 47 (2011) 4147–4149.
[22] Y.S. Kwon, I.Y. Song, J. Lim, S.H. Park, A. Siva, Y.C. Park, H.M. Jang, T. Park, RSC Adv. 2 (2012) 3467–3472.
[23] Z.P. Zhang, S.M. Zakeeruddin, B.C. O'Regan, R. Humphry-Baker, M. Grätzel, J. Phys. Chem. B 109 (2005) 21818–21824.
[24] T. Horiuchi, H. Miura, K. Sumioka, S. Uchida, J. Am. Chem. Soc. 126 (2004) 12218–12219.
[25] S.Y. Bang, M.J. Ko, K. Kim, J.H. Kim, I.-H. Jang, N.-G. Park, Synth. Met. 162 (2012) 1503–1507.
[26] A. Allegrucci, N.A. Lewcenko, A.J. Mozer, L. Dennany, P. Wagner, D.L. Officer, K. Sunahara, S. Mori, L. Spiccia, Energy Environ. Sci. 2 (2009) 1069–1073.
[27] R.H. Williams, L.A. Hamilion, J. Am. Chem. Soc. 74 (1952) 5418–5420.
[28] L. Hu, S. Dai, J. Weng, S. Xiao, Y. Sui, Y. Huang, S. Chen, F. Kong, X. Pan, L. Liang, K. Wang, J. Phys. Chem. B 111 (2007) 358–362.
[29] E.S. Gawalt, G. Lu, S.L. Bernasek, J. Schwartz, Langmuir 15 (1999) 8929–8933.
[30] K. Zhu, N.R. Neale, A. Miedaner, A.J. Frank, Nano Lett. 7 (2007) 69–74.
[31] Z. Ning, Y. Fu, H. Tian, Energy Environ. Sci. 3 (2010) 1170–1181.
[32] Y. Bai, J. Zhang, D. Zhou, Y. Wang, M. Zhang, P. Wang, J. Am. Chem. Soc. 133 (2011) 11442–11445.
[33] F. Fabregat-Santiago, J. Bisquert, G. Garcia-Belmonte, G. Boschloo, Sol. Energy Mater. Sol. Cells 87 (2005) 117–131.